Vol 11 No 10 June 2002
/2002/11(10)/
Chinese Physics
2002 Chin. Phys.Soc.
and IOP Publishing Ltd

A Design of Novel Type SC Magnet for Super-High field fMRI by using Harmonic Analysis Method of Magnetic Vector Potentials

Zu Donglin(俎栋林), Guo Hua(郭华)，Song Xiaoyu(宋枭禹), Bao Shanglian(包尚联)
Institute of Heavy Ion Physics, Physics College，Peking University, Beijing 100871，China
(Received 16 March 2002;revised manuscript 25 April 2002)

The approach of magnetic scalar potential expanded in a series of Legendre polynomials is suitable for designing conventional superconducting MRI magnet of distributed solenoidal configuration, whereas the approach of magnetic vector potential expanded in associate-Legendre harmonics is suitable to design a single-solenoid magnet that has multiple tiers, in which each tier may have multiple layers with different winding lengths. A set of three equations to suppress some of the lowest higher order harmonics is found. As an example a 4-Tesla single-solenoid MRI magnet with 4×6 layers of SC wires is designed. The degree of homogeneity in 0.5m diameter sphere volume (DSV) is better than 5.8 ppm. The same degree of homogeneity is retained after optimal integralization of turns in each correction layer. The ratio B_m / B_0 in the single-solenoid magnet is 30% lower than that in the conventional six-solenoid magnet. This tolerates higher rated SC current in the coil. The Lorentz force of the coil in the single-solenoid system is also much lower than in the six-solenoid system. This novel type of magnet possesses significant advantage over conventional ones, especially when used as a super-high field fMRI magnet.

Keywords: super-high field SC magnet for fMRI, high homogeneity fMRI magnet, **single-solenoid type fMRI magnet, magnetic vector potential, harmonic analysis approach, end correction**

PACC: 0755 8760I 4110F 7470P

1. Introduction

Magnetic resonance imaging (MRI) scanner is a powerful non-invasive imaging tool that produces cross-sectional tomographic and three dimensional images. It provides more information than other imaging tools since MR signal depends on a multitude of tissue parameters such as proton density ρ, longitudinal relaxation time T1, transverse relaxation time T2, chemical shift δ, diffusion coefficient D, diffusion tensor $\vec{\vec{D}}$, etc. Novel MRI parameters such as single quantum coherences (SQCs), double quantum coherences (DQCs), multiple quantum coherences (MQCs),[1] intermolecular multiple quantum coherences (IMQCs),[1] etc. have been proposed. Clinical MRI scanners typically have field strengths no stronger than 2.0T (open to 3.0T now according to FDA), but those used for research such as human brain functional magnetic resonance imaging (fMRI) require higher field strengths in order to get better SNR and better resolution. FMRI scanners with 4T, 7T, 8T field strengths have already been working, while the10T system is under plan. The superconducting (SC) main magnet is a key component of an fMRI scanner. It costs over a half of an fMRI scanner.

The conventional MRI SC magnet has distributed-solenoid structure[2,3] such as the six-coil system.[4] The magnetic field in the central zone of the magnet is analyzed by means of magnetic scalar potentials[5-7] expanded in spherical harmonics. We propose a single-solenoid structure with 4 tiers. There are 6 layers in each tier as shown in Fig.1. The residual field error is reached to over the 9th

[1*] Project supported in part by the National Natural Science Foundation of China(Grant No. 19675005)

harmonics. Our strategy is to expand the magnetic vector potential instead of the magnetic scalar potential.[8]

2. Formulation

The magnetic vector potential[9,10] produced by the current carrying solenoid is

$$A_\varphi = \mu_0 nI_0 \sum_{q=0}^{\infty} \frac{1}{(2q+1)(2q+2)} \frac{r^{2q+1}}{R^{2q}} P_{2q+1}^1(\cos\theta) \bullet \int_{\alpha_0}^{\pi/2} P_{2q+1}^1(\cos\alpha)\sin^{2q}\alpha \, d\alpha , \quad (1)$$

where μ_0 is the permeability in vacuum, n the turn density, I_0 the current in the solenoid winding, $P_{2q+1}^1(x)$ the associated Legendre polynomials, R and L the inner radius and the half-length of the main solenoid, respectively, and $\alpha_0 = \arctan(R/L)$. For convenience, we use a function $F^{(q)}(\alpha)$ to represent the integral item in Eq.(1):

$$F^{(q)}(\alpha) = \int_{\alpha_0}^{\pi/2} P_{2q+1}^1(\cos\alpha)\sin^{2q}\alpha \, d\alpha . \quad (2)$$

Thus the Eq. (1) can be rewritten as

$$A_\varphi = \mu_0 nI_0 \sum_{q=0}^{\infty} \frac{1}{(2q+1)(2q+2)} \frac{r^{2q+1}}{R^{2q}} P_{2q+1}^1(\cos\theta) F^{(q)}(\alpha) . \quad (3)$$

To obtain each order of harmonics of the magnetic vector potentials, $A_\varphi^{(q)}$, we only need to calculate the integral $F^{(q)}(\alpha)$ for each tier. Then Eq. (2) should be substituted as

$$F^{(q)}(\alpha) = \int_{\alpha_{0i}}^{\alpha_i} P_{2q+1}^1(\cos\alpha)\sin^{2q}\alpha \, d\alpha = F^{(q)}(\alpha_i) - F^{(q)}(\alpha_{0i}) , \quad (4)$$

here the subscript "i" indicates the tier number, i=0 means the main tier of the solenoid, and i=1,2,3 denote the successive correction tiers. The central magnetic field B_0 is the zero-th order harmonic

$$B_0 = B_z^{(0)} = \mu_0 nI_0 \left(\sum_{i=0}^{3} \cos\alpha_{0i} - \sum_{i=1}^{3} \cos\alpha_i\right) , \quad (5)$$

The other higher order harmonics are as follows:

$$B_z^{(1)} = \frac{\mu_0 nI_0}{2} r^2 [3\cos\theta P_3(\cos\theta) + \sin\theta P_3^1(\cos\theta)] \bullet [\sum_{i=1}^{3} R_i^{-2} F^{(1)}(\alpha_i) - \sum_{i=0}^{3} R_i^{-2} F^{(1)}(\alpha_{0i})] , \quad (6)$$

$$B_z^{(2)} = -\frac{3\mu_0 nI_0}{8} r^4 [5\cos\theta P_5(\cos\theta) + \sin\theta P_5^1(\cos\theta)] \bullet [\sum_{i=1}^{3} R_i^{-4} F^{(2)}(\alpha_i) - \sum_{i=0}^{3} R_i^{-4} F^{(2)}(\alpha_{0i})] , \quad (7)$$

$$B_z^{(3)} = \frac{\mu_0 nI_0}{16} r^6 [7\cos\theta P_7(\cos\theta) + \sin\theta P_7^1(\cos\theta)] \bullet [\sum_{i=1}^{3} R_i^{-6} F^{(3)}(\alpha_i) - \sum_{i=0}^{3} R_i^{-6} F^{(3)}(\alpha_{0i})] ; \quad (8)$$

where R_i is the radius of the i-th tier.

From Eqs. (6), (7) and (8) it is easy to see that in order to nullify the 3rd, 5th and 7th harmonics, we have to solve the set of three equations as below:

$$\begin{cases} \sum_{i=1}^{3} R_i^{-2} F^{(1)}(\alpha_i) - \sum_{i=0}^{3} R_i^{-2} F^{(1)}(\alpha_{0i}) = 0, \\ \sum_{i=1}^{3} R_i^{-4} F^{(2)}(\alpha_i) - \sum_{i=0}^{3} R_i^{-4} F^{(2)}(\alpha_{0i}) = 0, \\ \sum_{i=1}^{3} R_i^{-6} F^{(3)}(\alpha_i) - \sum_{i=0}^{3} R_i^{-6} F^{(3)}(\alpha_{0i}) = 0. \end{cases} \quad (9)$$

Here α_i are the unknown variables to be found. We can determine precisely the length of the i-th correction tier by α_i values. If there is only one layer in each tier, we call it a "single-layer" solenoid magnet, which is only capable of generating 1.0 tesla or so field strength. In order to get higher field strength such as 2 to 10 tesla, the "multi-layer" solenoid magnet structure must be taken into account. IF there are N layers in each tier, the Eq. (9) should be replaced by

$$\begin{cases} \sum_{i=1}^{3}\sum_{j=0}^{N-1} R_{ij}^{-2} F^{(1)}(\alpha_i) - \sum_{i=0}^{3}\sum_{j=0}^{N-1} R_{ij}^{-2} F^{(1)}(\alpha_{0ij}) = 0, \\ \sum_{i=1}^{3}\sum_{j=0}^{N-1} R_{ij}^{-4} F^{(2)}(\alpha_i) - \sum_{i=0}^{3}\sum_{j=0}^{N-1} R_{ij}^{-4} F^{(2)}(\alpha_{0ij}) = 0, \\ \sum_{i=1}^{3}\sum_{j=0}^{N-1} R_{ij}^{-6} F^{(3)}(\alpha_i) - \sum_{i=0}^{3}\sum_{j=0}^{N-1} R_{ij}^{-6} F^{(3)}(\alpha_{0ij}) = 0; \end{cases} \quad (10)$$

where α_{0ij}=arctan(R_{ij}/L), α_{ij}=arctanR_{ij}/(L-L_{ij}), R_{ij} and L_{ij} are the radius and the length of the j-th layer (j=0 to N-1) in the i-th tier (i=0,1,2,3), respectively. As soon as α_i is found through solving equations (10), the central field strength B_0 can be calculated using

$$B_0 = \mu_0 n I_0 (\sum_{i=0}^{3} \sum_{j=0}^{N-1} \cos\alpha_{0ij} - N \sum_{i=1}^{3} \cos\alpha_i) . \quad (11)$$

The residual field error is dominated by the lowest nonzero higher order harmonics (HOHs) $B_z^{(4)}$ and $B_z^{(5)}$:

$$B_z^{(4)} = -\frac{\mu_0 n I_0}{128} r^8 [9\cos\theta P_9(\cos\theta) + \sin\theta P_9^1(\cos\theta)]$$
$$\bullet [\sum_{i=1}^{3} \sum_{j=0}^{N-1} R_{ij}^{-8} F^{(4)}(\alpha_i) - \sum_{i=0}^{3} \sum_{j=0}^{N-1} R_{ij}^{-8} F^{(4)}(\alpha_{0ij})] , \quad (12)$$

$$B_z^{(5)} = \frac{\mu_0 n I_0}{256} r^{10} [11\cos\theta P_{11}(\cos\theta) + \sin\theta P_{11}^1(\cos\theta)]$$
$$\bullet [\sum_{i=1}^{3} \sum_{j=0}^{N-1} R_{ij}^{-10} F^{(5)}(\alpha_i) - \sum_{i=0}^{3} \sum_{j=0}^{N-1} R_{ij}^{-10} F^{(5)}(\alpha_{0ij})] . \quad (13)$$

3.Design

We designed a 4-Tesla single solenoid magnet as shown in Fig.1. It consists of a main tier and three correction tiers.[11] In each tier there are 6 layers of conducting wire (see Fig.1). The conducting wire is 1.07mm- diameter insulated SC wire. There is a 3mm-thick insulating sheet with bores in it for liquid Helium to pass through between adjacent layers. The SC wire selected is standard and commercially available, such as C84-3.3C NbTi filamentary copper matrix wire provided by GEC Alsthom. Each layer of the main tier has 2056 turns. So the total length of the magnet is 2L=2.19992m. The radius of each layer in each tier can be expressed as

R_{ij}=[50+1.542i+j(even)×0.407/2]cm, (14a)

R_{ij}={50+1.542i+[j(odd)-1]×0.407/2}cm, (14b)

where j(even) means j=0,2,4; j(odd) means j=1,3,5. Substituting these values of R_{ij} and α_{0ij} into Eqs.(10) and taking N=6 there, then solving the set of the three equations, we obtain the three real roots α_1, α_2 and α_3. Thus the lengths of each layer in each correction tier can be precisely determined. The data for details are listed in Table 1.

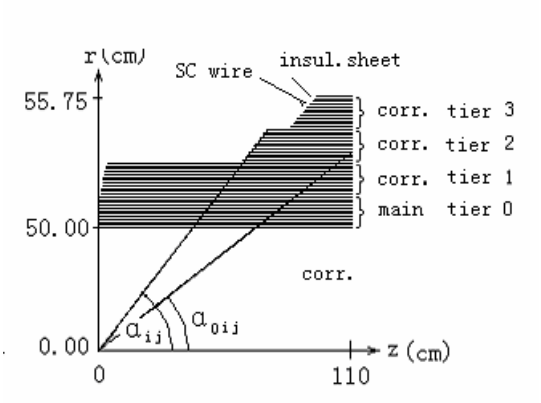

Fig.1 The sturcture of 4-T single-solenoid fMRI magnet. only one quadrant of the section is shown.

4. Results

The values of α_i obtained through solving equations (10) are listed in the 4th column of Table 1. The central magnetic induction B_0=4 Tesla, the theoretical homogeneity dominated by the 9th and the 11th order of harmonics is better than 5.8ppm. However, the ideal number of turns in each layer (see the 5th column of the Table 1) corresponding to the ideal angle α_i is not an integer in general. In manufacturing a magnet, it is necessary to make the number of turns an integer. Thus an "integralization of turns" treatment is required. The integralization of turns in each layer results in a corresponding inner-end-angle α_{ij} instead of the α_i. But the α_{ij} no longer satisfies exactly the equation-set (10) in general. Thus the 3rd, 5th and 7th harmonics reappear and thereby make a significant contribution to the inhomogeneity. Therefore the field homogeneity is determined by

$$\frac{\Delta B}{B_0} = \sum_{q=1}^{5} B_z^{(q)} / B_0 . \quad (15)$$

To calculate the q-th harmonic component $B_z^{(q)}$, the corresponding factors $F^{(q)}(\alpha)$ in Eqs. (6), (7), (8), (12) and (13) should be replaced by

$$\sum_{i=1}^{3} \sum_{j=0}^{5} R_{ij}^{-2q} F^{(q)}(\alpha_{ij}) - \sum_{i=0}^{3} \sum_{j=0}^{5} R_{ij}^{-2q} F^{(q)}(\alpha_{0ij}) . \quad (16)$$

If integralizing the turns of each layer N_{ij} to the adjacent integer, the homogeneity deteriorates as much as 50 ppm (see the 6th column of Table 1). By making Eq.(15) extremely minimum using a mathematical program, a set of optimal integral numbers of turns N_{ij} (the 7th column of Table 1) which corresponds a set of α_{ij} (the 8th column of Table 1) can be found, such that the homogeneity or uniformity is kept still better than

5.8ppm. The comparison between the uniformity after integralization and the ideal homogeneity is shown in Fig.2.

As well known, the allowed current of a SC solenoid coil, i.e. the rated SC current depends on the maximum magnetic field B_m in its winding.

Table 1: The data of the 4-Tesla single solenoid magnet designed for fMRI

No. of tier	No. of Layer	Outer-end -angle α_{0ij} (rad)	Theoretical inner-end angle α_i (rad)	Ideal turn Number N_{ij} (half length)	To the nearest whole number N_{ij}(halflength)	Optimal N_{ij}(half length)	Corresp. optimal α_{ij} (rad)
Main tier (0)	0	0.426641	1.57079633	1028.00	1028	1028	1.570796
	1	0.427447		1028.00	1028	1028	1.570796
	2	0.430507		1028.00	1028	1028	1.570796
	3	0.431310		1028.00	1028	1028	1.570796
	4	0.434359		1028.00	1028	1028	1.570796
	5	0.435159		1028.00	1028	1028	1.570796
First corr. tier(1)	0	0.438198	1.56955581	1027.40	1028	1028	1.570796
	1	0.438995		1027.40	1027	1028	1.570796
	2	0.442022		1027.40	1027	1028	1.570796
	3	0.442817		1027.40	1027	1028	1.570796
	4	0.445833		1027.39	1027	1026	1.566726
	5	0.446625		1027.39	1027	1026	1.566734
Second corr. tier (2)	0	0.449630	0.57588856	263.94	264	264	0.575926
	1	0.450419		262.40	262	262	0.575652
	2	0.453414		256.54	257	257	0.576162
	3	0.454199		255.00	255	255	0.575889
	4	0.457183		249.14	249	249	0.575806
	5	0.457966		247.60	248	246	0.574953
Third corr. tier (3)	0	0.460938	0.53691000	170.32	170	170	0.536746
	1	0.461718		168.64	169	170	0.537607
	2	0.464680		162.25	162	162	0.536784
	3	0.465457		160.57	161	161	0.537128
	4	0.468407		154.18	154	154	0.536820
	5	0.469181		152.50	153	151	0.536159
homogeneity				5.8ppm	50ppm	5.8ppm	

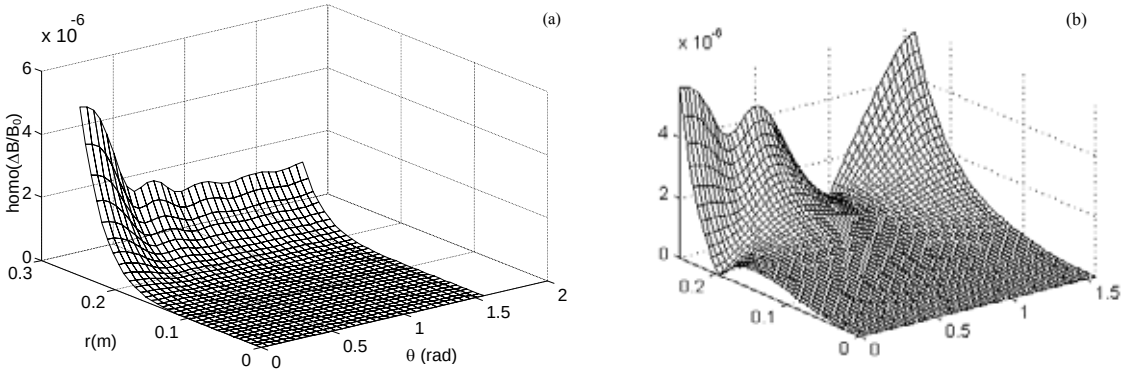

Fig.2. For the 4-T single-solenoid magnet designed for fMRI, the comparison between the ideal homogeneity (a) and the homogeneity determined by the optimal integralization of turn numbers (b).

. The ratio B_m / B_0 is related to the geometry of a magnet. For the single-solenoid magnet designed here, the $B_m / B_0 < 1.39$. However, the B_m / B_0 is greater than 2.0 in a conventional distributed- solenoid magnet such as the six-coil system.

5. Discussions

That our single-solenoid fMRI magnet structure uses three correction tiers each including multiple layers to annul the 3rd, 5th and 7th HOHs, and to develop a highly homogeneous field is feasible. An optimal set of integers of turns which keeps the homogeneity within the limit of theoretical homogeneity can be found. If using 4×15 layers instead of 4×6 layers here, the overall field strength will reach to 10 tesla while the same homogeneity can be kept. Furthermore, an active shielded fMRI magnet system can be constructed using two proposed single solenoid coils, one inside the other coaxially, the outer coil being used as the bucking coil which satisfies the requirement that the net magnetic moment of the composite equals to zero when viewed from a distance much greater than the radius of the magnet bore.[12]

In summary, the single solenoid structure proposed here possesses two outstanding advantages over the conventional distributed -solenoid structure. Firstly it gets rid of the tremendous Lorentz force between the separated windings. The huge force can cause the coil windings to be deformed to result in a bad deviation from the theoretical homogeneity unless using particularly heavy supports. Secondly, the ratio B_m / B_0 in a single-solenoid magnet is significantly lower than that in a distributed -solenoid magnet. Thereby relatively larger rated current is allowed in the former. The higher the working magnetic field, the more serious the problems of both the Lorentz force and the ratio B_m / B_0 become. The conventional fMRI magnet will drastically increase in cost with increasing field strength. Therefore the great potential of the single-solenoid fMRI magnet will make it more attractive.

References

[1] Zheng S K, Chen Z, Chen Z W and Zhong J H 2001 Chin. Phys. 10 558

[2] Murphy M F 1989 IEEE Mag-25(2) 1755

[3] Bobrov E S, et al 1987 IEEE Mag-23(2) 3

[4] Zhang Y, Han S, Feng Z X 1989 IEEE Mag-25(2) 1881

[5] Girard B and Sauzade M 1964 NIM 25 269

[6] Garrett M W 1967 J. of Appl. Phys. 38(6) 2563

[7] Anderson W A 1961 Rev. Sci. Instr. 32(3) 241

[8] Jackson J D 1976 Classical Electrodynamics, New York: wiley.

[9] Yu F C, Zheng C K 1992 Electrodynamics, Peking University Press

[10] Roomeo F, Hoult D I 1984 Magnetic Resonance in Medicine 1 44

[11] Zu D L, Guo H, et al 1997 Proc. MT-15, 903, Beijing

[12] Green M A, Carolan J 1987 IEEE Mag-23(2), 1299

（上接第 155 页）用 ^{131}I-BDI-1 对荷瘤裸鼠进行放射免疫治疗，显示 ^{131}I-BDI-1 对膀胱癌有明显的抑制作用，其治疗后第 4 周对肿瘤的抑制率达 99%。免疫毒素对膀胱癌细胞体外杀伤试验证明免疫毒素可有效杀伤肿瘤细胞，用 BDI-1 与苦瓜毒素偶联物对 18 例膀胱癌患者及用 BDI-1 与蓖麻毒素偶联物对 31 例膀胱癌患者术后进行膀胱灌注导向治疗，表明免疫毒素在清除膀胱内小于 1cm 的小瘤灶及防止术后复发方面有明显疗效。

结论

1．^{131}I、^{99m}Tc 及 ^{188}Re-抗膀胱癌单克隆抗体 BDI-1 及免疫毒素具有良好的免疫活性，在生物体内可很好地定位于膀胱癌组织。

2．膀胱灌注放射免疫显像由于标记抗体不进入血液直接与肿瘤组织结合，具有肿瘤定位快、无人体免疫反应、影像清晰与全身毒性小等优点，有可能成为膀胱癌诊断的无创伤性的新手段，特别是对膀胱早期肿瘤、膀胱原位癌、行膀胱镜检困难的患者的诊断具有良好的应用前景。

3．对膀胱癌影像进行定量分析可提高诊断灵敏度，有助于膀胱肿瘤早期诊断；同时，定量分析可对膀胱癌进行初步分级诊断。

4．采用多体位放射免疫显像可对膀胱癌进行精确定位。

5．放射免疫显像采用双核素减影法处理对输尿管癌的诊断有潜在的应用价值。

6．膀胱灌注导向治疗在预防膀胱癌术后复发中可能有良好的应用前景。